Published in final edited form as:
Neuroimage. 2010 July 1; 51(3): 1117–1125. doi:10.1016/j.neuroimage.2010.01.083.

Microstructural connectivity of the arcuate fasciculus in adolescents with high-functioning autism

P. Thomas Fletcher[a,b,c,*], **Ross T. Whitaker**[a,b,c], **Ran Tao**[a,b], **Molly B. DuBray**[d], **Alyson Froehlich**[g], **Caitlin Ravichandran**[j,k], **Andrew L. Alexander**[e,f], **Erin D. Bigler**[c,g,h,i], **Nicholas Lange**[j,k], and **Janet E. Lainhart**[c,d,g,h]

[a] School of Computing, University of Utah, Salt Lake City, UT, USA

[b] Scientific Computing and Imaging Institute, University of Utah, Salt Lake City, UT, USA

[c] The Brain Institute at the University of Utah, Salt Lake City, UT, USA

[d] Interdepartmental Program in Neuroscience, University of Utah, Salt Lake City, UT, USA

[e] Waisman Laboratory for Brain Imaging and Behavior, Waisman Center, Madison, WI, USA

[f] Departments of Medical Physics, University of Wisconsin, Madison, WI, USA

[g] Department of Psychiatry, University of Utah, Salt Lake City, UT, USA

[h] Department of Radiology, University of Utah, Salt Lake City, UT, USA

[i] Department of Psychology and Neuroscience, Brigham Young University, Provo, UT, USA

[j] Departments of Psychiatry and Biostatistics, Harvard University, Cambridge, MA, USA

[k] Neurostatistics Laboratory, McLean Hospital, Belmont, MA, USA

Abstract

The arcuate fasciculus is a white matter fiber bundle of great importance in language. In this study, diffusion tensor imaging (DTI) was used to infer white matter integrity in the arcuate fasciculi of a group of subjects with high-functioning autism and a control group matched for age, handedness, IQ, and head size. The arcuate fasciculus for each subject was automatically extracted from the imaging data using a new volumetric DTI segmentation algorithm. The results showed a significant increase in mean diffusivity (MD) in the autism group, due mostly to an increase in the radial diffusivity (RD). A test of the lateralization of DTI measurements showed that both MD and fractional anisotropy (FA) were less lateralized in the autism group. These results suggest that white matter microstructure in the arcuate fasciculus is affected in autism and that the language specialization apparent in the left arcuate of healthy subjects is not as evident in autism, which may be related to poorer language functioning.

Keywords

Diffusion tensor imaging; Arcuate fasciculus; Autism

[*]Corresponding author. Warnock Engineering Building, 72 South Campus Central Dr., Room 3750, Salt Lake City, UT, 84112, USA. Fax: +1 801 585 6513. fletcher@sci.utah.edu (P.T. Fletcher).

Introduction

Impairments in language development and functioning are striking in autism. Onset of spoken language is often significantly delayed and approximately one-third of individuals with autism never develop functional use of language. Response to spoken language is sometimes so profoundly impaired during early childhood that some children with autism seem deaf even though their hearing is normal. Comprehension of simple or complex language is deficient. When language does develop, deviant and unusual forms of language may occur. Rapid processing and production of fluent, flexible, and appropriate social language, so important in interacting with others, may never fully develop. Despite the striking nature of the language phenotype in autism at all stages of development, little is known about the brain basis of this fundamental feature.

The arcuate fasciculus (AF) is a white matter fiber bundle of great importance to language. This white matter tract connects the classical cortical language regions: Wernicke's area in the posterior superior temporal gyrus, Broca's area in the inferior frontal gyrus, and the recently confirmed Geschwind's area in the inferior parietal lobule (Catani et al., 2005). The need for communication between these cortical regions for language function makes the AF an important structure to examine in autism. Research suggests that structural and functional abnormalities exist in language-related cortex in autism.

Most studies examining the brain basis of language abnormalities in autism have focused on cortical regions. In vivo neuroimaging shows atypical volumetric hemispheric asymmetry in Broca's area (De Fosse et al., 2004; Herbert et al., 2002; Tager-Flusberg and Joseph, 2003). Although volumetric differences are absent in the superior temporal gyrus (STG), some individuals with autism show disruption of the typical structure–function relationship STG gray matter volume and receptive language function (Bigler et al., 2007). In addition, differences in the diffusion properties of STG white matter microstructure and asymmetry have been found (Lee et al., 2007). Postmortem studies have found abnormalities in the minicolumns of the temporal and frontal lobes (Casanova et al., 2002, 2003) and, in some cases, cortical dysgenesis, including abnormally enlarged and hyperconvoluted temporal lobes, cortical thickening, disturbed cortical laminar pattern, and many scattered neurons in the white matter in the STG (Bailey et al., 1998).

Research concerning the relationship between classical cortical language areas in autism, while sparse, is suggestive of impairment. For example, children with autism show reduced correlations between gray matter volumes in frontal and temporal language regions compared to controls (McAlonan et al., 2005). Further, functional connectivity between Wernicke's and Broca's areas is decreased during sentence comprehension (Just et al., 2004). However, lacking from imaging and postmortem studies of autism to date is examination of the AF, the brain structure critical for communication between language cortices and ultimately language development and functioning.

Abnormal development of the AF could be linked to the language impairment found in autism. The direct segment of the AF connects Broca's and Wernicke's areas. The indirect segment connects these two areas to Geschwind's area in the inferior parietal lobule (Catani et al., 2005). Lesions in parts of the direct pathway in adults result in conduction aphasias characterized by impaired repetition, especially passive, non-semantically based repetition, but relatively preserved spontaneous speech and language comprehension (Catani et al., 2005). Lesions in the indirect pathway in adults result in transcortical motor aphasias characterized by relatively intact passive repetition but impaired spontaneous speech and/or comprehension. Although the indirect pathway might be more impaired in verbal individuals with autism than the direct pathway given the frequency of immediate echolalia during early childhood, we

chose to begin our examination of the AF in autism with the direct pathway. The classic direct pathway is anatomically the most validated and understood, and almost nothing is known about its development and structure in autism.

Diffusion tensor imaging (DTI) allows researchers to use microstructural features to examine anatomy, volume, density, and asymmetry of white matter pathways including the AF. Many DTI studies show left lateralized asymmetry in volume and relative fiber density of the direct segment of the AF during typical development (Barrick et al., 2007; Eluvathingal et al., 2007; Glasser and Rilling, 2008; Nucifora et al., 2005; Parker et al., 2005; Powell et al., 2006; Vernooij et al., 2007). Left lateralized asymmetry in fractional anisotropy (FA) has also been found using DTI in typical adults (Catani et al., 2007; Powell et al., 2006). Typically developing adults have a correlation between FA asymmetry and aspects of their language functioning (Catani et al., 2007; Powell et al., 2006). Absence of typical leftward FA asymmetry is found in adults with schizophrenia (Kubicki et al., 2005) and children with developmental delay (Sundaram et al., 2008). These findings highlight the need to understand how the AF is organized and develops in individuals with autism and other disorders of language.

Diffusion tensor imaging (DTI) measures the direction and extent of microscopic water diffusion in the brain. Diffusion is affected by microstructure and is greatest in the direction of least restriction. A number of different histological components and features of white matter can affect water diffusion in tracts including axon cell membranes and myelin, tract architecture including fiber width, density and coherence, glial cells, and general “health” of axons in contrast to pathology that may affect them. White matter tracts are most commonly “dissected” out of diffusion tensor images by using tractography, which measures the net direction of axonal fibers in a given voxel and adjacent voxels and creates probabilistic maps of streamlines. Tractography results in exquisite anatomic images of white matter tracts, but to date, it has not easily allowed quantitative study of the microstructure of white matter within and along a tract.

Recent advances in DTI data analysis provide new powerful methods to examine the microstructure of white matter tracts during life. In this study, we use a novel mathematical method to volumetrically “dissect out” the direct segment of the AF. We then quantitatively measure features of white matter microstructure in the tract as a whole and along the length of the tract in both the right and left hemispheres. We examine and compare the microstructure of the direct segment of the AF in high-functioning adolescents with autism and matched typically developing controls. We hypothesized that participants with autism would show evidence of decreased microintegrity of the AF compared to controls. We predicted that case–control differences would be greater in the left than in the right AF and that differences in the AF would be greater than expected for average total brain white matter FA and MD. We also hypothesized that within the autism group, severity of language impairment would quantitatively be related to the degree of change in white matter microstructure.

Materials and methods

Participant ascertainment, diagnosis, and assessment

Ten high-functioning males with autism who had functional use of language were compared to 10 typically developing males. The two groups were matched on age, full scale IQ, verbal IQ, performance IQ, handedness, and head circumference. The majority of autism and all control participants were ascertained from the community; a minority of the autism subjects were recruited from social skills groups.

Autism was diagnosed using the Autism Diagnostic Interview (ADI-R) and Autism Diagnostic Observation Scale (ADOS-G) (Lord et al., 1994, 2000). All autism participants met ADI-R,

ADOS-G, DSM-IV-TR, and ICD-10 criteria for autistic disorder. Autism was idiopathic in all cases. Medical causes of autism were excluded by history, observation, karyotype, and Fragile×gene testing and participants with seizures were excluded. Typical development was confirmed in controls by history, direct assessment with ADOS-G, and IQ and language testing. Head circumference (HC) was measured using the methods of Farkas (1994).

IQ was measured using the Differential Abilities Scale (DAS) (Elliott, 1990), Wechsler Intelligence Scale for Children (WISC), or Wechsler Adult Intelligence Scale WAIS (Wechsler, 1991, 1997). For those participants receiving the DAS, verbal ability was used as a surrogate for VIQ, and nonverbal composite (nonverbal reasoning and spatial ability) as a surrogate for PIQ. Language was measured using the Clinical Evaluation of Language Functioning (CELF-3) (Semel et al., 1995). The CELF-3 is a comprehensive test of higher order expressive and receptive language function that includes subtests for semantics, grammar, syntax, and working memory for language. It is the language test most frequently used to assess children with autism and identifies language-based subgroups.

Diffusion tensor imaging

DTI data were acquired on a Siemens Trio 3.0-T Scanner with an 8-channel, receive-only head coil. DTI was performed using a single-shot, spin-echo, EPI pulse sequence, and SENSE parallel imaging (undersampling factor of 2). Diffusion-weighted images were acquired in twelve non-collinear diffusion encoding directions with diffusion weighting factor b=1000 s/mm^2 in addition to a single reference image (b ~0) (Hasan et al., 2001). Data acquisition parameters included the following: contiguous (no-gap) fifty 2. 5-mm-thick axial slices with an acquisition matrix of 128×128 over a FOV of 256 mm (2×2 mm^2 in-plane resolution), 4 averages, repetition time (TR)=7000 ms, and echo time (TE)=84 ms.

Eddy current-related distortion and head motion of each data set were corrected using an automatic image registration program (Rohde et al., 2004). Distortion-corrected DW images were interpolated to 1×1×1.25 mm^3 voxels, and six tensor elements were calculated using a multivariate log–linear regression method (Basser et al., 1994). The tensor upsampling is done only for the purposes of numerical computations on the voxel grid; a finer grid results in higher numerical accuracy. Each tensor was then diagonalized to estimate the three eigenvectors $\lambda=(\lambda_1, \lambda_2, \lambda_3)$, sorted from largest to smallest, and the corresponding eigenvalues ($\mathbf{e}_1$, $\mathbf{e}_2$, $\mathbf{e}_3$). The eigenvalues were used to compute fractional anisotropy, $FA=[3\mathrm{Var}(\lambda)]/(\lambda^2_1 + \lambda^2_2 + \lambda^2_3)]^{1/2}$, i.e., the normalized standard deviation of the eigenvalues, mean diffusivity, $MD=(\lambda_1 +\lambda_2 +\lambda_3)/3$, axial diffusivity, $AD=\lambda_1$, and radial diffusivity, $RD=(\lambda_2 +\lambda_3)/2$ (Basser and Pierpaoli, 1996).

Diffusion tensor data processing and image analysis

We recently developed a novel method for volumetric segmentation and quantification of white matter fiber tracts (Fletcher et al., 2007). Our approach is based on minimal cost paths between two regions, where the cost is defined as an integral of the local cost for passing through the diffusion tensor data. The full diffusion tensor data are used in the local cost, with lowest cost being along the major eigendirection and highest cost along the perpendicular directions. Globally optimal solutions for the minimal paths are found by solving a Hamilton–Jacobi partial differential equation. Unlike previous front propagation methods for DT-MRI, we then solve for minimal cost from a second target region. The two solutions are then combined, giving the minimal cost through each voxel of paths restricted to travel between the two regions.

For quantitative analysis, our method offers several advantages over fiber tractography (Basser et al., 2000), where the major eigenvector field is integrated forward from an initial seed point. First, our method is more robust to imaging noise because the full diffusion tensor data are

used and global solutions are found, while tractography suffers from accumulated local errors in the integration of the noisy major eigenvector fields. Also, region-to-region analysis with conventional tractography is challenging, because there is no way to steer tracts from a seed point toward a particular target or destination region. Finally, volumetric representations of the white matter pathways are preferable for statistical analysis since the original image data are included rather than interpolated data along streamlines.

The automatic volumetric segmentation of the AF requires as input a manual delineation of the endpoint regions of the tract in the DTI. Manual regions of interest (ROI) were outlined in a color image of the major diffusion tensor eigenvector (red=left/right, green=anterior/posterior, blue=superior/inferior) using the ITK-SNAP tool (Yushkevich et al., 2006, http://www.itksnap.org). The frontal endpoint region was outlined in the most frontal coronal slice in which the main stem of the AF was visible. The temporal endpoint region was outlined in the most lateral sagittal slice where the AF was visible. The same seeding procedure was performed for left and right arcuate endpoint regions and was done blind to the diagnostic group. This ROI selection process is shown in Fig. 1.

Using the volumetric white matter tract analysis, we segmented both the left and right arcuate fasciculi for each subject. The resulting semi-automatic segmentation of the left AF for an individual in the control group is shown in Fig. 2. In each structure, we computed the average values for fractional anisotropy (FA), mean diffusivity (MD), axial diffusivity (AD), and radial diffusivity (RD). These averages were computed using only voxels from the original data, not interpolated values in the upsampled data. We tested the reliability of our manual endpoint delineation method in the left AF in 10 subjects. Two raters independently manually delineated the endpoints of the left AF, and we compared the resulting average values for FA, MD, AD, and RD by calculating classical intraclass correlation coefficients (ICC) from a one-way random effects model. The ICCs for the left AF are 0.9087 for both FA and MD, 1.0000 for AD, and 0.9732 for RD.

We computed a total brain white matter mask from each DTI by thresholding on FA (FA >=0.25), followed by a morphological close operation to fill single-voxel holes. An average value was computed for each diffusion measurement (FA, MD, AD, and RD) for the total white matter. The final data that were computed were lateralization indices for each of the four diffusion measurements in the AF. Each lateralization index was calculated as $2(x_l - x_r)/(x_l + x_r)$, where x_l denotes the average value for the left AF and $x_r$denotes the average value for the right AF.

Biostatistical analysis

To understand relationships between hemispheric asymmetries in AF microstructure and autism, we fit separate linear mixed effect (LME) models (Laird and Ware 1982; Lange and Laird 1989; Venables and Ripley 2002; Lange 2003) for each tensor measure: FA, MD, AD, and RD. LMEs accommodate correlation between repeated measurements of response variables by allowing random deviations of covariate effects for individuals (“random effects”) from covariate effects for the population. In our setting, random intercepts accommodated correlation between tensor measures from the right and left hemispheres of each subject.

Our predictors of primary interest in these models were diagnosis (autism or control), hemisphere (left or right), autism by hemisphere interaction, and age. The control group and the right hemisphere were chosen as reference categories, so that a significant main effect of diagnosis (autism) indicated a significant difference in mean tensor measure between autism and controls in the right hemisphere; a significant main effect of hemisphere (left) indicated a significant difference in mean tensor measure between the right and left hemisphere for controls; and a significant autism by hemisphere interaction indicated a significant difference

in asymmetry between autism and controls. We also tested for significant differences between autism and controls in the left hemisphere using alternate parameterizations.

For these models, we chose to control for total brain white matter diffusion measurements and handedness regardless of their statistical significance as predictors. Because we aimed to learn about the effects of our primary predictors on AF asymmetry independent of total brain white matter properties and handedness changes, we first sequentially removed the linear effects of these two predictors on the tensor measures, so that the outcomes of our models for autism, hemisphere, and age effects were the residuals from these two linear fits rather than the actual right and left hemisphere values. Finally, we considered the addition of remaining group-matching variables (listed in Table 1) as covariates if their inclusion improved model fit.

To test for differences in the association between AF microstructure hemispheric lateralization and language functioning in autism, we fit separate least-squares regression models for each tensor measure with CELF-III score as the outcome and autism, tensor scalar lateralization index, and autism by tensor scalar lateralization index interaction as predictors. These models controlled for total brain white matter measurements, handedness, and age for all four tensor measures and additional matching variables when their inclusion improved model fit.

We employed the Akaike Information Criterion (AIC) (Akaike 1974), a tool for model selection that balances precision with simplicity, to determine whether the inclusion of matching variables improved the fit of our models. Maximum global false positive error rate was set at 0.05 for each test. Bonferroni corrections for testing multiplicity of tensor measures were applied; these corrections were overly conservative because the estimated tensor scalars are not statistically independent.

Results

Participant characteristics

Table 1 shows the characteristics of the case and control samples. There were no significant differences between the groups on age, VIQ, PIQ, handedness, or head circumference. As expected, the autism group showed impairment in language functioning as measured by the CELF-3.

Arcuate fasciculus volume

The AF was successfully segmented in both the left and right hemisphere for all autism and typically developing subjects in the study. The average total volume of the left AF (570±186 mm^3) was significantly greater than the average total volume of the right AF (222±101 mm^3) in the pooled sample including both groups (t=7.435, $p<10^{-5}$). We found age to have no significant effect on the volume of the left or right AF in either group, or on the asymmetry index of AF volume. There were no significant differences in left or right AF volumes between the autism and control groups. The differences were also not significant when age, age by diagnosis, and total white matter volume covariates were included. The raw volume data are plotted in Fig. 3.

Arcuate fasciculus microstructure and hemispheric asymmetry of microstructure

Table 2 contains a summary of our raw data, being group means and SD by hemisphere for each tensor scalar summary without normalization by the hemispheric sum (as in asymmetry index). These data are also plotted in Fig. 4. In the autism group, note a possible loss of L > R asymmetry in FA and a loss of R > L asymmetry in MD and RD. Table 3 contains a summary of the global white matter tensor measurements. Differences in global white matter between

the two groups were tested in a linear model with age and age by diagnosis as covariates, as this gave the best AIC model fit, and the resulting *p*-values were Bonferroni corrected.

In the linear mixed models with hemisphere as the repeated measure, we first adjusted the DT-MRI summary measures linearly for the effects of the average diffusion summary measure in total brain white matter. Total brain white matter MD, AD, and RD had statistically significant effects on the corresponding measures in the AF: MD: $p<10^{-4}$; AD: $p=0.0008$; RD: $p<10^{-5}$, Bonferroni corrected. Handedness, however, did not have a statistically significant effect on any of the AF measures.

Results from the LMEs are shown in Tables 4–6. Each table row contains the estimated effect of a covariate and its standard error (SE), the *t*-ratio of the two, and the associated Bonferroni corrected *p*-value. Table 4 shows a large and significant main effect of hemisphere ($p=0.015$), indicating increased FA in the left hemisphere (LH) for typically developing controls, and a significant increase in FA with age ($p=0.031$). For MD and RD, there are significant decreases in the LH for normal controls ($p<10^{-5}$ MD; $p<10^{-4}$ RD) that are nearly absent in autism ($p=0.002$ MD; $p=0.016$ RD Autism×LH interaction), Tables 5 and 6. For both MD and RD, there are non-significant decreases with age, though the decrease for RD approaches significance ($p=0.054$). There were no significant effects of autism, hemisphere, their interaction, or age on AD in the AF; this table is not present.

Arcuate fasciculus microstructure and language functioning

We tested for group differences in the relationships between asymmetries of arcuate fasciculus FA, MD, AD, and RD and language functioning as assessed by CELF-3. There were no differences in the associations of any of the hemispheric asymmetries with language functioning between autism and typically developing controls. Using models without autism by asymmetry interactions but controlling for diagnosis, there were also no significant associations between any of the hemispheric asymmetries and language functioning across diagnostic groups. When the two groups were pooled and diagnosis was not included as a covariate, there was a significant negative correlation between RD lateralization and language functioning ($t=-2.673$, $p=0.0167$). As discussed in the next section, this correlation must be interpreted carefully. By mixing the two groups, it is not possible to determine whether the correlation represents a general relationship between language and RD lateralization or whether there is a specific effect due to impairment of the AF in autism. However, this does point to the need for further study to investigate this relationship.

Discussion

A novel method for volumetric segmentation and quantification of white matter fiber tracts shows atypical arcuate fasciculus microstructure and hemispheric asymmetry in autism. Mean diffusivity and radial diffusivity are increased in the left arcuate fasciculus in the autism sample. The lack of asymmetry of these measures of white matter microstructure is also atypical: the rightward asymmetry in mean diffusivity and radial diffusivity seen in controls is absent in the autism group. Case–control differences are not found in fractional anisotropy or axial diffusivity. Arcuate fasciculus microstructure appears to be specifically affected in autism; the differences are not simply a result of brain-wide changes.

The arcuate fasciculus in typical development

The AF, successfully segmented in both hemispheres in all of our subjects, has patterns of asymmetry of size and microstructure similar to results of most published reports. In our typical adolescents, the AF has leftward asymmetry of volume and FA, rightward asymmetry of MD and RD, and symmetrical AD. Diffusion tensor tractography has been used to make maps of

reconstructed segments, measure relative fiber density, number of streamlines, and tract volume as indices of left and right AF size (Nucifora et al., 2005; Powell et al., 2006; Catani et al., 2007; Vernooij et al., 2007; Lebel and Beaulieu, 2009). All of these studies find that the AF in the left hemisphere is larger than in the right hemisphere in about 90% of individuals. Left lateralization is often extreme: the right AF cannot be reconstructed at all with tractography in over a third of typically developing children and adults (Catani et al., 2007; Lebel and Beaulieu, 2009). Rarely is this the case with the left AF. All studies examining FA in the direct segment of the AF find robust leftward lateralization in the majority of older children and adults (Buchel et al., 2004; Powell et al., 2006; Catani et al., 2007; Eluvathingal et al., 2007; Lebel and Beaulieu, 2009). Lateralization of MD, AD, and RD has not been well studied. In contrast to our findings of increased rightward MD and RD asymmetry of the AF in our control subjects, another study of children 6–17 years of age found greater leftward MD, RD, and AD asymmetry of the AF (Eluvathingal et al., 2007). However, tests of statistical significance are not reported.

Our findings also suggest continued age-related maturation of the AF during later childhood and adolescence. FA increases and RD decreases with cross-sectional age in our typical controls. The effects are present even when age-related changes in these DTI measures in the whole brain are removed. MD, AD, and the AF volume appear age-invariant in the age range of the children in our cross-sectional analysis, although caution is warranted given the sample size. These findings add to existing evidence of continued maturation of the left AF during childhood and adolescence, such as significant positive correlations of cross-sectional age and white matter density in the area of the left AF using voxel-based morphometry (Paus et al., 1999; Guo et al., 2007) and age-related increase in FA in the left AF using voxel-based analysis of DTI (Schmithorst et al., 2002). Results have not always been consistent, however. Age-related decreases in AF MD, AD, and RD have been found without an increase in FA (Eluvathingal et al., 2007), and a study using whole-brain voxel-based analysis found increasing FA and AD with age but no change in MD or RD in the left AF (Ashtari et al., 2007).

The arcuate fasciculus in autism

Pathology of the AF in our autism sample is evident in white matter microstructure and asymmetry of microstructure but not in volume. Volume of the AF and leftward volumetric asymmetry are similar in case and controls. MD and RD of the AF are significantly increased in autism particularly in the left hemisphere. There are no significant changes in FA or AD. This lack of changes may appear to conflict with the raw data shown in Fig. 4, where there appears to be possible group differences in AD and FA asymmetry. However, the lack of significance indicates that the differences are possibly explained by global white matter properties (included as a covariate), that is, they are not specific to the AF. The correction of AF tensor measurements by global white matter measurements demonstrates that abnormalities that are significant in the AF in autism are above and beyond any differences in the microstructure of the global white matter. It is also important that the most striking differences in the autism group are the significant decreases in AF tensor measurement asymmetries (MD and RD). These asymmetry differences are stronger than differences in the left AF alone, and they are stronger than the differences in global white matter, which are not statistically significant (Table 3).

What changes in white matter could result in such findings? This pattern of results is likely the manifestation of complex microstructural changes. From a simplistic point of view, if an increase in MD and RD was due merely to a decrease in myelination, we would expect to find smaller volume and decreased FA of the AF, which was not found in the autism group. Increased MD and RD mainly due to decreased axonal density (a decrease in the number of axons in the AF with an increase in intra-axonal space) might spare volume and AD but should

decrease FA. The latter was not found in our study. An increase in the mean width of axons in the AF, in the absence of other changes, would likely result in similar findings. Increased MD and RD mainly due to a decrease in the organization of fibers or more tortuosity may not affect volume but should increase RD and decrease FA and AD, a pattern not found in the autism sample. Abnormal DTI microstructure of the left AF in the absence of volumetric change may be the structural correlate of decreased functional connectivity between Wernicke's and Broca's areas found in fMRI studies of language processing in autism (Just et al., 2004; Knaus et al., 2008).

The arcuate fasciculus and language functioning

We did not find the expected clinico-pathological relationship between atypical microstructure of the direct temporo-frontal segment of the AF and language functioning. However, this was not surprising as all of the autism participants in our study were verbal and the sample sizes were too small to detect anything other than a very large language effect. Further investigation with a larger sample size is needed to sufficiently test this hypothesis. We do believe that it is appropriate to test this hypothesis in a group of individuals with high-functioning autism, who do show a significant decrease in language function compared to controls, as can be seen in the CELF-3 data in Table 1. Also, the variability of CELF-3 and tensor measurements in the high-functioning autism group is large. Therefore, it is reasonable to expect that if there are autism-specific deficits in language resulting from microstructural impairments of the AF, these relationships would be present in a high-functioning group. Our analysis did find a general negative trend in the pooled sample between CELF-3 and RD lateralization in the AF. However, the statistical significance disappeared with inclusion of the group diagnosis as a covariate. The mixed sample result cannot be interpreted directly since the trend may be due to a general relationship between the AF and language or due to autism-specific impairments in the AF. It does indicate the need for further investigation with a larger sample size to determine the nature of the relationship between the AF and language impairment in autism.

Another possibility for future investigation of the relationship between language functioning and the arcuate fasciculus would be to use language tests more specific to the function of the AF. The CELF-3 is a comprehensive test of higher order expressive and receptive language function that includes subtests for semantics, grammar, syntax, and working memory for language. It is the language test most frequently used to assess children with autism and identifies language-based subgroups. Although the CELF-3 is a reasonable albeit general first step in the examination of clinical correlates of AF microstructure in autism, language tests, such as tests of repetition (Breier et al., 2008), that assess functions more specific to the direct segment of the AF (Catani et al., 2005), may be more informative.

Potential neurobiological implications

The changes in microstructure of the AF suggested by our findings could be due to a number of different processes. First, since autism is a developmental disorder with onset in early childhood, the microstructural changes may be a persisting manifestation of a primary abnormality of early development of the AF. The microstructural changes in the AF could be secondary to primary cortical maldevelopment, such as abnormal development of cortical minicolumns (Casanova et al., 2009). It is also possible that the observed changes are the result of abnormal language functioning and expertise rather than a cause (Paus et al., 1999). Continued maturation in white matter microstructure of the AF during late neurodevelopment in typically developing young people and age-related changes in white matter microstructure observed in our study raise important questions. For example, can specific interventions improve pathology of microstructure and language functioning in individuals with autism during the protracted period of AF development?

The novel methods used in this study

Our study includes several methodological advances. The first advance is a new method for volumetric segmentation and quantification of white matter fiber tracts. In contrast to the use of tractography to reconstruct the AF, the novel methods we used successfully segmented both the left and right AF in all autism and control subjects. This success may be due to the fact that the volumetric segmentation algorithm is more robust to image noise than tractography and that it is a globally optimal solution between the endpoint regions. These advantages result in the ability to segment white matter tracts with lower anisotropy, and thus more ambiguity in the tensor direction, as is the case in the right AF.

The second advance is in the linear mixed models, which offer two advantages. First, the AF DT-MRI summary measures are adjusted for the effects of the average diffusion summary measure in total brain white matter. This adjustment allows us to conclude that significant differences between the groups are specific to the AF and not due to global differences in white matter microstructure. Second, the asymmetry in diffusion measurements in the left and right AF are treated as within-subject random effects. This has the advantage over a statistical analysis of an asymmetry index in that the errors in both hemispheres can be explicitly modeled, which improves the statistical power.

Limitations of the study

Our study was limited to high-functioning males with autism. The benefit of the sample was decreased variability due to heterogeneity in autism that could decrease statistical power and confound the results. Use of a high-functioning verbal sample, however, made it less likely we would find significant differences between the groups. However, we do not know if the findings will generalize to females, cognitively lower functioning and non-verbal individuals with autism, and very young children.

The cross-sectional nature of the sample and relatively small sample sizes make the age-related findings inconclusive. Other comparison groups including young people with other developmental disorders are needed to test the specificity of the results to autism.

Finally, we only examined the direct segment of the AF. In future work, we will investigate the efficacy of the volumetric DTI analysis in segmenting the indirect segments of the AF and how these segments are affected in autism. Finally, the volumetric DTI segmentation algorithm is limited by the need to manually define the endpoints of the white matter tract. While our analysis of multiple raters shows that this can be done reliably, it is likely that manual raters are unable to include all projections of the AF into the cortex. We are also exploring the possibility of seeding the algorithm with cortical parcelations from registered structural MRI or seeding with activation areas in fMRI language tasks.

Conclusions

We have presented a study of the white matter integrity of the AF in autism using a new volumetric DTI analysis method. Our results indicate that white matter microstructure, as measured by RD and MD, of the left AF is abnormal in autism. An absense of lateralization in MD and FA in the autism group indicates a lack of the typical leftward specialization of language functioning in terms of white matter connectivity. Future work using a larger sample size will investigate longitudinal analysis of white matter development in the AF and correlations of diffusivity measurements with language function.

Acknowledgments

This work was supported by Autism Speaks Mentor-based Postdoctoral Fellowship #2291(J.E.L. for P.T.F.) and Predoctoral Fellowship #1677 (J.E.L. for M.B.D.) Awards; NIMH RO1 MH084795 and MH080826 (J.E.L.), the National Alliance for Medical Image Computing (NAMIC; R.T.W.), NIH Grant U54 EB005149 (R.T.W.), University of Utah Multidisciplinary Research Seed Grant (P.T.F. and J.E.L.), and NIDCD F31 DC010143 (M.B.D.). Additional support came from NIH Mental Retardation/Developmental Disabilities Research Center (MRDDRC, Waisman Center; A.L.A.), NIMH 62015 (A.L.A.), NIDA15879 (A.L.A.); NINDS R01 NS34783 (N.L.), NIMH P50 MH60450 (N.L.), and NICHD U19 HD35476 (University of Utah CPEA). The content is solely the responsibility of the authors and does not necessarily represent the official views of the NIMH, NIDCD, NICHD, NINDS, NIDA, or the National Institutes of Health.

We acknowledge Drs. Jeffrey Lu, William McMahon, Judith Miller, and Hilary Coon, Michael South, and Nicanas Garcia, along with Michael Johnson, Jubel Morgan, Barbara Young, Tracy Abildskov, and other members of the Utah Autism Research Program. We thank Henry Buswell and Melody Johnson of the University of Utah Center for Advanced Imaging Research. We express our sincere gratitude to the children and adults who participated in this study and their families.

References

Akaike H. A new look at the statistical model identification. IEEE Trans Automat Contr 1974;19:716–723.

Ashtari M, Cervellione KL, Hasan KM, Wu J, McIlree C, Kester H, Ardekani BA, Roofeh D, Szeszko PR, Kumra S. White matter development during late adolescence in healthy males: a cross-sectional diffusion tensor imaging study. NeuroImage 2007;35:501–535. [PubMed: 17258911]

Bailey A, Luthert P, Dean A, Harding B, Janota I, Montgomery M, Rutter M, Lantos P. A clinicopathological study of autism. Brain 1998;121:889–905. [PubMed: 9619192]

Barrick TR, Lawes IN, Mackay CE, Clark CA. White matter pathway asymmetry underlies functional lateralization. Cereb Cortex 2007;17:591–598. [PubMed: 16627859]

Basser PJ, Mattiello J, LeBihan D. MR diffusion tensor spectroscopy and imaging. Biophys J 1994;66:259–267. [PubMed: 8130344]

Basser PJ, Pajevic S, Pierpaoli C, Duda J, Aldroubi A. In vivo fiber tractography using DT-MRI data. Magn Reson Med 2000;44:625–632. [PubMed: 11025519]

Basser PJ, Pierpaoli C. Microstructural and physiological features of tissues elucidated by quantitative-diffusion-tensor MRI. J Magn Reson B 1996;111:209–219. [PubMed: 8661285]

Bigler ED, Mortensen S, Neeley ES, Ozonoff S, Krasny L, Johnson M, Lu J, Provencal SL, McMahon W, Lainhart JE. Superior temporal gyrus, language function, and autism. Dev Neuropsychol 2007;31:217–238. [PubMed: 17488217]

Breier JI, Hasan KM, Zhang W, Men D, Papanicolaou AC. Language dysfunction after stroke and damage to white matter tracts evaluated using diffusion tensor imaging. Am J Neuroradiol 2008;29:483–487. [PubMed: 18039757]

Buchel C, Raedler T, Sommer M, Sach M, Weiler C, Koch MA. White matter asymmetry in the human brain: a diffusion tensor MRI study. Cereb Cortex 2004;14:945–951. [PubMed: 15115737]

Casanova MF, Buxhoeveden DP, Switala AE, Roy E. Minicolumnar pathology in autism. Neurology 2002;58:428–432. [PubMed: 11839843]

Casanova MF, Buxhoeveden D, Gomez J. Disruption in the inhibitory architecture of the cell minicolumn: implications for autism. Neuroscientist 2003;9:496–507. [PubMed: 14678582]

Casanova MF, El-Baz A, Mott M, Mannheim G, Hassan H, Fahmi R, Giedd J, Rumsey JM, Switala AE, Farag A. Reduced gyral window and corpus callosum size in autism: possible macroscopic correlates of a minicolumnopathy. J Autism Dev Disord 2009;39:751–764. [PubMed: 19148739]

Catani M, Allin MP, Husain M, Pugliese L, Mesulam MM, Murray RM, Jones DK. Symmetries in human brain language pathways correlate with verbal recall. Proc Natl Acad Sci U S A 2007;104:17163–17168. [PubMed: 17939998]

Catani M, Jones DK, Ffytche DH. Perisylvian language networks of the human brain. Ann Neurol 2005;57:8–16. [PubMed: 15597383]

De Fosse L, Hodge SM, Makris N, Kennedy DN, Caviness VS Jr, McGrath L, Stelle S, Ziegler DA, Herbert MR, Frazier JA, Tager-Flusberg H, Harris GJ. Language-association cortex asymmetry in autism and specific language impairment. Ann Neurol 2004;56:757–766. [PubMed: 15478219]

Elliott, CD. Differential Ability Scales: Introductory and Technical Handbook. The Psychological Corporation; New York: 1990.

Eluvathingal TJ, Hasan KM, Kramer L, Fletcher JM, Ewing-Cobbs L. Quantitative diffusion tensor tractography of association and projection fibers in normally developing children and adolescents. Cereb Cortex 2007;17:2760–2768. [PubMed: 17307759]

Farkas, LG. Anthropometry of the Head and Face. 2. Raven Press; New York: 1994.

Fletcher PT, Tao R, Jeong WK, Whitaker RT. A volumetric approach to quantifying region-to-region white matter connectivity in diffusion tensor MRI. Inform Process Med Imaging (IPMI), LNCS 2007;4584:346–358.

Glasser MF, Rilling JK. DTI tractography of the human brain's language pathways. Cereb Cortex 2008:2471–2482. [PubMed: 18281301]

Guo X, Chen C, Chen K, Jin Z, Peng D, Yao L. Brain development in Chinese children and adolescents: a structural MRI study. Neuroreport 2007;18:875–880. [PubMed: 17515793]

Hasan KM, Parker DL, Alexander AL. Comparison of gradient encoding schemes for diffusion-tensor MRI. J MRI 2001;13:769–780.

Herbert MR, Harris GJ, Adrien KT, Ziegler DA, Makris N, Kennedy DN, Lange NT, Chabris CF, Bakardjiev A, Hodgson J, Takeoka M, Tager-Flusberg H, Caviness VS Jr. Abnormal asymmetry in language association cortex in autism. Ann Neurol 2002;52:588–596. [PubMed: 12402256]

Just MA, Cherkassky VL, Keller TA, Minshew NJ. Cortical activation and synchronization during sentence comprehension in high-functioning autism: evidence of underconnectivity. Brain 2004;127:1811–1821. [PubMed: 15215213]

Knaus TA, Silver AM, Lindgren KA, Hadjikhani N, Tager-Flusberg H. fMRI activation during a language task in adolescents with ASD. J Int Neuropsychol Soc 2008;14:967–979. [PubMed: 18954477]

Kubicki M, Park H, Westin CF, Nestor PG, Mulkern RV, Maier SE, Niznikiewicz M, Connor EE, Levitt JJ, Frumin M, Kikinis R, Jolesz FA, McCarley RW, Shenton ME. DTI and MTR abnormalities in schizophrenia: analysis of white matter integrity. NeuroImage 2005;26:1109–1118. [PubMed: 15878290]

Laird NM, Ware JH. Random-effects models for longitudinal data. Biometrics 1982;38:963–974. [PubMed: 7168798]

Lange N, Laird NM. The effect of covariance structure on variance estimation in balanced growth curve models with random parameters. J Am Stat Assoc 1989;84:241–247.

Lange N. What can modern statistics offer imaging neuroscience? Stat Methods Med Res 2003;12:447–469. [PubMed: 14599005]

Lebel C, Beaulieu C. Lateralization of the arcuate fasciculus from childhood to adulthood and its relation to cognitive abilities in children. Hum Brain Mapp 2009:3563–3573. [PubMed: 19365801]

Lee JE, Bigler ED, Alexander AL, Lazar M, DuBray MB, Chung MK, Johnson M, Morgan J, Miller JN, McMahon WM, Lu J, Jeong EK, Lainhart JE. Diffusion tensor imaging of white matter in the superior temporal gyrus and temporal stem in autism. Neurosci Lett 2007;424:127–132. [PubMed: 17714869]

Lord C, Risi S, Lambrecht L, Cook E, Leventhal BL, DiLavore PC, Pickles A, Rutter M. The autism diagnostic observation schedule-generic: a standardized measure of social and communicative deficits associated with the spectrum of autism. J Autism Dev Disord 2000;30:205–223. [PubMed: 11055457]

Lord C, Rutter M, Le Couteur A. Autism Diagnostic Interview–Revised: a revised version of a diagnostic interview for caregivers of individuals with possible pervasive developmental disorders. J Autism Dev Disord 1994;24:659–685. [PubMed: 7814313]

McAlonan GM, Cheung V, Cheung C, Suckling J, Lam GY, Tai KS, Yip L, Murphy DG, Chua SE. Mapping the brain in autism. A voxel-based MRI study of volumetric differences and intercorrelations in autism. Brain 2005;128:268–276. [PubMed: 15548557]

Nucifora PG, Verma R, Melhem ER, Gur RE, Gur RC. Leftward asymmetry in relative fiber density of the arcuate fasciculus. Neuroreport 2005;16:791–794. [PubMed: 15891571]

Parker GJ, Luzzi S, Alexander DC, Wheeler-Kingshott CA, Ciccarelli O, Lambon Ralph MA. Lateralization of ventral and dorsal auditory-language pathways in the human brain. NeuroImage 2005;24:656–666. [PubMed: 15652301]

Paus T, Zijdenbos A, Worsley K, Collins DL, Blumenthal J, Giedd JN, Rapoport JL, Evans AC. Structural maturation of neural pathways in children and adolescents: in vivo study. Science 1999;283:1908–1911. [PubMed: 10082463]

Powell HW, Parker GJ, Alexander DC, Symms MR, Boulby PA, Wheeler-Kingshott CA, Barker GJ, Noppeney U, Koepp MJ, Duncan JS. Hemispheric asymmetries in language-related pathways: a combined functional MRI and tractography study. NeuroImage 2006;32:388–399. [PubMed: 16632380]

Rohde GK, Barnett AS, Basser PJ, Marenco S, Pierpaoli C. Comprehensive approach for correction of motion and distortion in diffusion-weighted MRI. Magn Reson Med 2004;51:103–114. [PubMed: 14705050]

Schmithorst VJ, Wilke M, Dardzinski BJ, Holland SK. Correlation of white matter diffusivity and anisotropy with age during childhood and adolescence: a cross-sectional diffusion-tensor MR imaging study. Radiology 2002;222:212–218. [PubMed: 11756728]

Semel, E.; Wiig, EH.; Secord, WA. Clinical Evaluation of Language Fundamentals. 3. The Psychological Corporation; San Antonio, TX: 1995.

Sundaram SK, Sivaswamy L, Makki MI, Behen ME, Chugani HT. Absence of arcuate fasciculus in children with global developmental delay of unknown etiology: a diffusion tensor imaging study. J Pediatr 2008;152:250–255. [PubMed: 18206698]

Tager-Flusberg H, Joseph RM. Identifying neurocognitive phenotypes in autism. Philos Trans R Soc Lond B Biol Sci 2003;358:303–314. [PubMed: 12639328]

Venables, VN.; Ripley, BD. Modern Applied Statistics with S. 4. Springer-Verlag; 2002.

Vernooij MW, Smits M, Wielopolski PA, Houston GC, Krestin GP, van der Lugt A. Fiber density asymmetry of the arcuate fasciculus in relation to functional hemispheric language lateralization in both right- and left-handed healthy subjects: a combined fMRI and DTI study. NeuroImage 2007;35:1064–1076. [PubMed: 17320414]

Wechsler, D. Wechsler Intelligence Scale for Children. 3. The Psychological Corporation; San Antonio, TX: 1991. (WISC-III)

Wechsler, D. Wechsler Adult Intelligence Scale. 3. The Psychological Corporation; San Antonio, TX: 1997. (WAIS-III)

Yushkevich PA, Piven J, Hazlett HC, Smith RG, Ho S, Gee JC, Gerig G. User-guided 3D active contour segmentation of anatomical structures: significantly improved efficiency and reliability. NeuroImage 2006;31:1116–1128. [PubMed: 16545965]

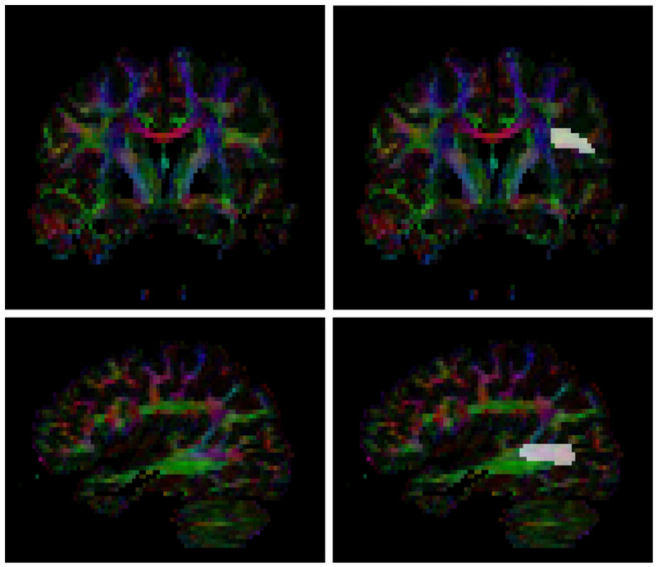

Fig. 1.
An example of the manual endpoint region selection. The selected frontal region is shown on the top, and the selected temporal region is shown on the bottom.

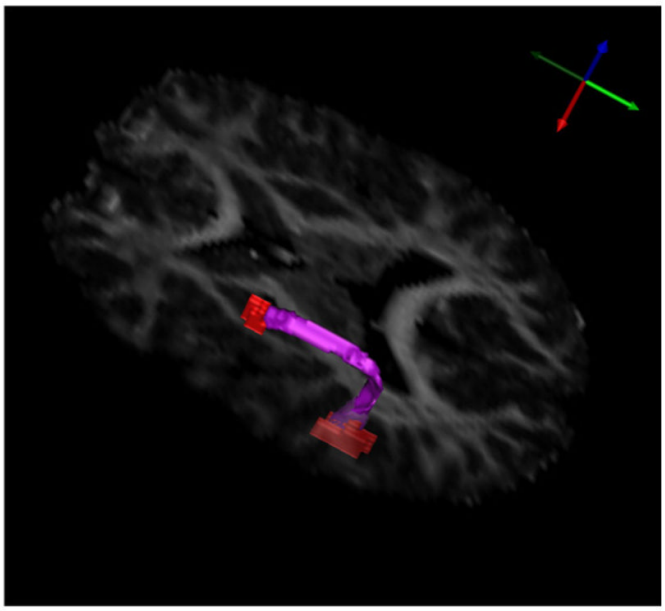

Fig. 2.
The arcuate fasciculus segmented automatically from an individual in the control group. Shown in red are the manually delineated seed regions.

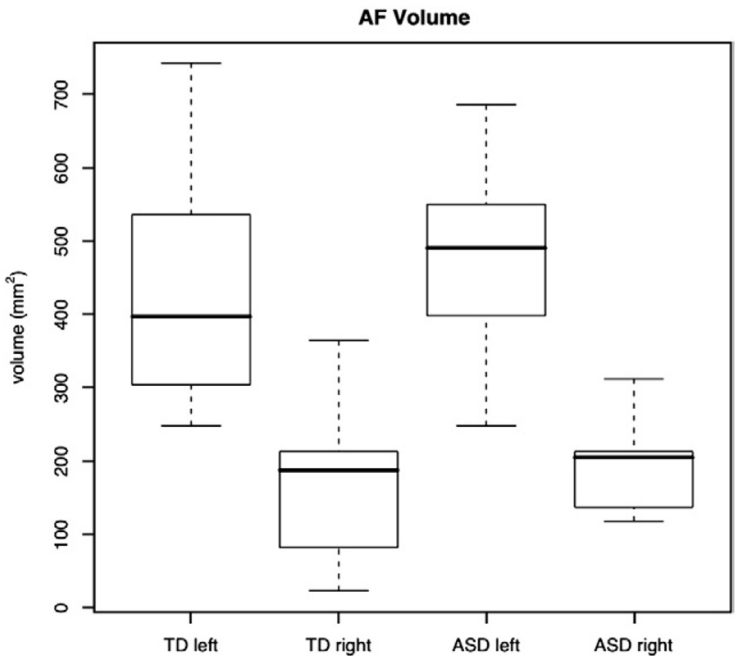

Fig. 3.

Boxplot of the left and right AF volume for both typically developing and autism groups. Center bold lines denote median values, boxes show middle 50%, whiskers show extent, and circles denote outliers.

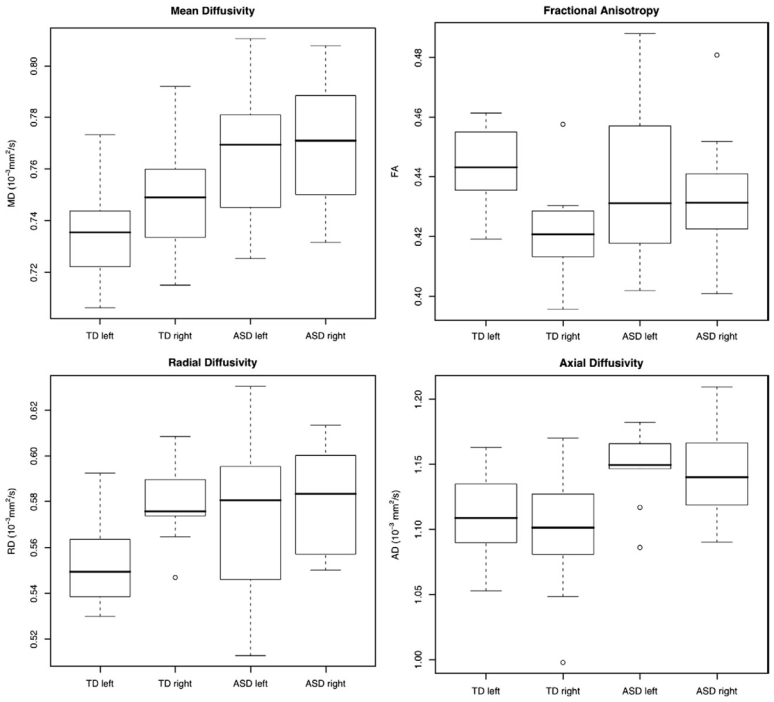

Fig. 4.

Boxplots of MD (top left), FA (top right), radial diffusivity (bottom left), and axial diffusivity (bottom right) in the left arcuate fasciculus for both typically developing and autism groups.

Table 1

Participant variables employed for group-matching and language data.

	Typically developing (*n*=10)			Autism (*n*=10)			Group comparison	
	Mean	**SD**	**Range**	**Mean**	**SD**	**Range**	**F**	***p*-Value**
Age (years)	13.36	1.34	11–16	14.25	1.92	11–17	1.47	0.241
PIQ	112.50	14.80	94–131	108.80	13.90	91–135	0.332	0.572
VIQ	102.7	9.52	92–125	103.7	18.55	70–131	0.023	0.881
Handedness	81.30	14.34	60–100	80.60	19.07	53–100	0.0086	0.927
HC (cm)	55.67	1.58	53–58	54.95	1.83	53–59	0.889	0.358
CELF-3	104.80	10.28	93–125	87.80	19.79	50–111	5.812	0.027

Table 2

Summary statistics for each tensor scalar in the AF by diagnostic group and hemisphere (mean, SD). ASD, autism spectrum disorder subjects. TD, typically developing controls. Δ_G =column-wise mean difference, ASD − TD. Δ_H =row-wise mean difference, L − R.

Fractional anisotropy (FA)				**Mean diffusivity (MD, 10^{-3} mm^2/s)**			
	L	**R**	**Δ_H**		**L**	**R**	**Δ_H**
ASD	0.437 (0.027)	0.434 (0.022)	0.004	ASD	0.766 (0.026)	0.768 (0.024)	−0.002
TD	0.444 (0.013)	0.422 (0.016)	0.022	TD	0.737 (0.020)	0.753 (0.024)	−0.015
Δ_G	−0.006	0.011		Δ_G	0.029	0.016	
Axial diffusivity (AD, 10^{-3} mm^2/s)				Radial diffusivity (RD, 10^{-3} mm^2/s)			
	L	R	Δ_H		L	R	Δ_H
ASD	1.15 (0.029)	1.14 (0.039)	0.00	ASD	0.576 (0.033)	0.580 (0.024)	−0.005
TD	1.11 (0.034)	1.10 (0.050)	0.01	TD	0.552 (0.019)	0.579 (0.017)	−0.027
Δ_G	0.04	0.05		Δ_G	0.024	0.001	

Table 3

Summary statistics for the global white matter tensor scalars (mean and SD). Test statistics are adjusted for age and diagnosis by age interactions.

	TD	ASD	*t*	*p*-value
FA	0.425 (0.0065)	0.418 (0.0094)	−2.02	0.244
MD (10^{-3} mm^2/s)	0.818 (0.016)	0.828 (0.018)	2.15	0.189
AD (10^{-3} mm^2/s)	1.22 (0.021)	1.23 (0.019)	1.61	0.508
RD (10^{-3} mm^2/s)	0.618 (0.015)	0.628 (0.019)	2.38	0.121

Table 4

Linear mixed effects model analysis of FA, adjusted for total brain white matter FA, handedness, and head circumference (LH, left hemisphere).

Covariate	Est. Effect	SE	*t*-value	*p*-value
Autism	0.016	0.007	2.33	0.133
LH	0.022	0.006	3.34	0.015
Autism×LH	−0.018	0.009	−1.94	n.s.
Age (years)	0.005	0.002	3.04	0.03

Table 5

Linear mixed effects model analysis of MD, adjusted for total brain white matter MD and handedness. Units for the estimated effect size and standard error are $10^{-}3$ mm^2/s. (LH=left hemisphere).

Covariate	Estimated effect	SE	*t*-value	*p*-value
Autism	0.006	0.005	1.10	n.s.
LH	−0.015	0.005	−6.91	$<10^{-5}$
Autism×LH	0.013	0.003	4.15	0.002
Age (years)	−0.002	0.001	−1.04	n.s.

Table 6

Linear mixed effects model analysis of RD adjusted for total brain white matter RD, handedness, and head circumference. Units for the estimated effect size and standard error are 10^{-3} mm^2/s (LH, left hemisphere).

Covariate	Estimated effect	SE	*t*-value	*p*-value
Autism	−0.008	0.006	−1.43	n.s.
LH	−0.027	0.005	−5.64	$<10^{-4}$
Autism×LH	0.022	0.007	3.31	0.016
Age (years)	−0.004	0.002	−2.78	0.054